International Journal of Mechanical, Industrial and Aerospace Sciences
ISSN: 2517-9950
Vol:6, No:8, 2012

3D Modeling of Temperature by Finite Element in Machining with Experimental Authorization

P. Mottaghizadeh, M. Bagheri

***Abstract*—**In the present paper, the three-dimensional temperature field of tool is determined during the machining and compared with experimental work on C45 workpiece using carbide cutting tool inserts. During the metal cutting operations, high temperature is generated in the tool cutting edge which influence on the rate of tool wear. Temperature is most important characteristic of machining processes; since many parameters such as cutting speed, surface quality and cutting forces depend on the temperature and high temperatures can cause high mechanical stresses which lead to early tool wear and reduce tool life. Therefore, considerable attention is paid to determine tool temperatures. The experiments are carried out for dry and orthogonal machining condition. The results show that the increase of tool temperature depends on depth of cut and especially cutting speed in high range of cutting conditions.

***Keywords*—**Finite element method, Machining, Temperature measurement, Thermal fields

I. Introduction

THE metal cutting is an intricate process. During the process, due to the plastic deformation and friction, heat generation occurs. It could be assumed that all the required cutting energy is converted to heat. The temperature increases in the cutting zone which can affect the material behavior and result in the formation of tool-chip. The maximum temperature which occurs at the tool-chip interface can increase fracture considerably. Many parameters such as cutting speed, surface quality and cutting forces depend on the temperature. Hence, determination of temperature distribution has been one of the major issues in the machining researches.

Temperature prediction is one of the most complex subjects in the metal cutting and is extremely difficult to develop an accurate temperature prediction model in machining. Due to the complexity of the contact phenomenon, temperature prediction is a quite challenge in the metal cutting process [1].

In order to obtain cutting forces, specific cutting energy and appropriate temperature for coated tool material, various models are simulated; then appropriate cutting condition which is very important is defined.

P. Mottaghizadeh is graduated of chemical engineering, Amirkabir University of Technology (Tehran Polytechnic), Tehran, Iran (phone: 912-483-5197; e-mail: p.mottaghizadeh@gmail.com).

M. Bagheri is a graduate student of mechanical engineering, Amirkabir University of Technology (Tehran Polytechnic), Tehran, Iran (e-mail: m.bagheri.mech@gmail.com).

Many studies on the prediction of cutting temperature are accomplished that present simulation of cutting forces, stresses and temperature fields on chip, tool and workpiece. Cases in point are analyzing rounded edge tools [2], analysis on the friction modeling in orthogonal machining [3], analyses the temperatures in hard turning [4] and Finite element modeling of temperature distribution in the cutting zone in turning processes with differently coated tools [5].

The primary effect of temperature is on tool wear. There are various tool wear mechanisms [6]. Furthermore, the tool longevity can be determined by the maximum temperature in the tool rake face. However, the maximum temperature and the temperature gradient effects can cause subsurface deformation, metallurgical structure change and mechanical properties alteration in the machined surface.

In the hard turning process, because of the high hardness of the workpiece materials, high temperatures and high mechanical stresses are created which lead to the early tool wear and reduce the longevity of tool; besides, they increase the forces and tensile residual stresses, affect the surface finish and cause white surface layer to damage [7]. Numerous attempts have been made to measure the temperature in the machining operations [8]. One of the most extensively used experimental techniques to measure the temperature in machining is the use of thermocouples.

A study through a finite elements model using the Abaqus™ code is conducted to predict the interface cutting temperature and its dependence to the crater wear mechanism [9].

Locating temperature measuring instruments much close to the cutting edge is very difficult. Due to the lack of experimental data verifying the proposed mathematical models, most published articles rely on the few published experimental data [10]. The infrared radiation technique (IR) is the second most used method of temperature measuring. In this case, the surface temperature of the body is measured based on its emitted thermal energy. In some cases the IR technique indicated lower temperatures than the thermocouple method did.

In this paper, temperature is measured with an infrared pyrometer during orthogonal cutting condition. Also, the effect of cutting speed, feed rate and depth of cut on the tool temperature (rake face) were considered.

Finally, by the use of experiments, an equation for estimating of tool temperature was developed.

II. Thermal Modeling

A. Heat balance

In order to solve the problem with finite element method (FEM), analytical solution of the problem was reviewed by choosing each element as a control volume. From the first law of thermodynamics, the rate of difference between thermal and mechanical energy entering and exiting the control volume summing to the rate of heat generation is equal to the rate of energy stored within the control volume. This principal can be written as

$$\dot{E}_{in} - \dot{E}_{out} + \dot{E}_{generated} = \dot{E}_{stored} \ . \tag{1}$$

B. Heat conduction

The rate of heat conduction to the control volume with the dimensions of dx, dy and dz from x, y and z directions, are called $\dot{Q}_x$, $\dot{Q}_y$ and $\dot{Q}_z$, respectively. The rate of heat conduction in three directions is defined as

$$\begin{aligned} \dot{Q}_x &= -kA\frac{\partial T}{\partial x} = -kdydz\frac{\partial T}{\partial x} \\ \dot{Q}_y &= -kA\frac{\partial T}{\partial y} = -kdxdz\frac{\partial T}{\partial y} \\ \dot{Q}_z &= -kA\frac{\partial T}{\partial z} = -kdxdy\frac{\partial T}{\partial z} \ . \end{aligned} \tag{2}$$

Here, k is the thermal conductivity and A is the area of the surface that is exposed to this heat conduction.

C. Heat convection

Another way of heat transfer is convection from the system to the surrounding air; the heat convection rate is directed from the control volume to the surrounding air which can be written as following.

$$\dot{Q}_{conv} = h_a A\left(T - T_\infty\right) \tag{3}$$

Here, h_a is the convection coefficient between the element and the ambient air flowing around. The temperature of ambient air is considered equal to the room temperature; therefore, room temperature is boundary condition. Some elements are not in contact with air so this term becomes zero for them.

D. Heat generation

The amount of generated heat depends on heat generation rate per control volume unit

$$\dot{E}_{generated} = \dot{q}dxdydz \ . \tag{4}$$

The values of generated heat are obtained from the force and velocity factors along shear and friction dimensions, as can be seen in following.

$$\dot{q}_s = F_s V_s = \frac{\tau h V \cos\left(\alpha_n\right)}{\sin\left(\alpha_n\right)\ \cos\left(\phi_n - \alpha_n\right)} \tag{5}$$

$$\dot{q}_f = F_f V_c = \frac{\tau h V \sin\left(\beta_n\right)}{\cos\left(\phi_n + \beta_n - a_n\right)\sin\left(\phi_n - a_n\right)} \tag{6}$$

In these equations, h is the uncut chip thickness which corresponds to feed rate in turning; V is the cutting velocity; τ is the shear flow stress; α_n, β_n and ϕ_n are the normal rake angle, normal friction angle and normal shear angle, respectively. The values of generated heat are per unit of cut; therefore, we can achieve the real values with multiplying them by depth of cut.

E. Heat stored

The amount of heat stored within the control volume depends on volume, density ρ, specific heat capacity C, and the rate of temperature change in the control volume.

$$\dot{E}_{stored} = \rho C\frac{\partial T}{\partial t}dxdydz \tag{7}$$

It is assumed that heat flows from all surrounding objects and enters to the control volume; therefore, the heat balance equation can written as follow.

$$\dot{Q}_x + \dot{Q}_y + \dot{Q}_z + \dot{Q}_{conv} + \dot{Q}dxdydz = \rho C\frac{\partial T}{\partial t}dxdydz \tag{8}$$

In (8), $\dot{Q}$ is defined as the following term.

$$\dot{Q} = \dot{q}_s + \dot{q}_f \tag{9}$$

F. Discretizition of heat equation by explicit method

The problem must be discretized in time. The integer p is introduced for this purpose, where $t = p\Delta t$ and the finite-difference approximate to the time derivative in equation is expressed as

$$\begin{aligned} \frac{\partial T}{\partial x} &= \frac{T^p_{i+1,j,k} - T^p_{i,j,k}}{\Delta t} \\ \frac{\partial T}{\partial y} &= \frac{T^p_{i,j+1,k} - T^p_{i,j,k}}{\Delta t} \\ \frac{\partial T}{\partial z} &= \frac{T^p_{i,j,k+1} - T^p_{i,j,k}}{\Delta t} \ . \end{aligned} \tag{10}$$

The superscript p denotes the time dependence of T; the time derivative is expressed in terms of temperature difference between the new $(p+1)$ and previous (p) times.

In the explicit method of solution, these temperatures are evaluated at the previous (p) time. Hence, Eq. 10 is considered to be a forward difference approximation to the time derivative. The accuracy of the finite difference solution may be improved by decreasing the values of nodal dimension and Δt.

An undesirable aspect of the explicit method is that it is not unconditionally stable. In order to prevent the explicit method from becoming unstable, the prescribed value of Δt must be maintained below a certain limit which depends on element dimensions and other parameters of the system.

G.Finite difference equation for tool

In this section, after meshing of the tool, a partial differential equation is derived for each element in this grid. Notice that in the selection of the element numbers, both accuracy and time are of great importance. In the present paper, the optimum element number with proper precision is used for temperature estimation. Differential equation for one type of the elements is as the following.

$$kA'\frac{\partial T}{\partial x}+kA''\frac{\partial T}{\partial y}+kA'''\frac{\partial T}{\partial z}+h_aA\left(T-T_\infty\right)=\rho CV\frac{\partial T}{\partial t} \tag{11}$$

This element is shown in Fig. 1 (highligheted element).

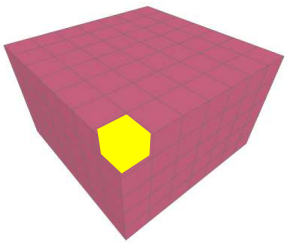

Fig. 1 Finite element modeling of insert

Here, it is assumed that element dimensions are $\Delta x=\Delta y=\Delta z$; hence, A', A'' and A''' are equal surfaces, $A=\frac{3l^2}{4}$, $A'=\frac{l^2}{4}$ and $V=\frac{l^3}{8}$; Substituting these terms in (11) in a small time interval, the following equation is obtained.

$$\frac{kl^2}{4}\left(\frac{T^p_{i+1,j,k}-T^p_{i,j,k}}{l}\right)+\frac{kl^2}{4}\left(\frac{T^p_{i,j+1,k}-T^p_{i,j,k}}{l}\right)+\frac{kl^2}{4}\left(\frac{T^p_{i,j,k+1}-T^p_{i,j,k}}{\Delta t}\right)+q\frac{3h_al^2}{4}=\frac{\rho Cl^3}{8}\left(\frac{T^{p+1}_{i,j,k}-T^p_{i,j,k}}{\Delta t}\right) \tag{12}$$

By solving the nodal temperature of the new $(p+1)$ time, the following is achieved.

$$T^{p+1}_{i,j,k}=\frac{2kt}{\rho Cl^2}\left(T^p_{i+1,j,k}+T^p_{i,j+1,k}+T^p_{i,j,k+1}\right)+q\frac{6t}{\rho Cl}+\left(1-\frac{6kt}{\rho Cl^2}\right)\left(T^p_{i,j,k}\right) \tag{13}$$

Here, some parameters are defined.

$$Fo=\frac{kt}{\rho Cl^2} \tag{14}$$

$$Bi=\frac{h_al}{k} \tag{15}$$

Fo is Fourier number and Bi is Biot number, and finally we have

$$T^{p+1}_{i,j,k}=2Fo\left(T^p_{i+1,j,k}+T^p_{i,j+1,k}+T^p_{i,j,k+1}+3\frac{ql}{k}\right)+\left(1-6\,Fo-6\,Fo\times Bi\right)T^p_{i,j,k}\ . \tag{16}$$

III. Experimental Validation

A. Tool and workpiece material

In both methods, IR and thermocouple, the qualification set-up is identical and metal removal is carried out by carbide tool with triangle insert and constant geometry, where is the rake angle 0, inclination angle 0, clearance angle 4, and entering angle 90 degrees on a C45 steel pipe (C45; carbon 0.25%, iron 98%, manganese 1.03%, silicon 0.28%, copper 0.2%, sulfur 0.05%, phosphorous 0.04%) with 110mm diameter and 5mm thickness. To enhance the accuracy and evenness of pipe thickness, the inside and outside of the pipe were machined on a conventional lathe. Hence, the required diameter and thickness with different desirable depth of cuts can be achieved. A schematic outline of insert is shown in Fig. 2.

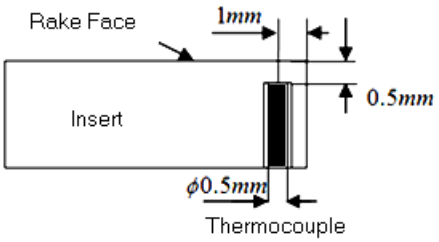

Fig. 2 The schematic outline of insert

A Phyfe model dynamometer with special tool-holder including embedded K-Type thermocouple was used so as to measure the cutting force, feed force and temperature.

The thermocouple diameter is 0.5mm. The temperature ranges from -30 to +700 degrees centigrade, the dimension is about $220 \times 60 \times 60$ mm and the weight is approximately 50N. Photos of (a) dynamometer and (b) tool-holder are shown in Fig. 3.

(a)

(b)

Fig. 3 The photos of (a) dynamometer and (b) tool-holder

B. Infrared pyrometer

The temperature signals were measured by an immobile, wholly digital and fast compact pyrometer for a calibrated temperature range of -3 to +900 degrees centigrade. The laser pilot lights direct the pyrometer to the measuring position. The size of the measurement spot was 0.3 mm, which corresponded to a distance to the measurement surface of 0.2 m. The pyrometer had a response time of 250 ms. Temperature of point A on the insert has been measured, as shown in Fig. 4. This position is alongside the leading edge at 1mm from the cutting edge so that the effect of chip obstruction during machining could be avoided. The pyrometer is calibrated by a k-Type-thermocouple.

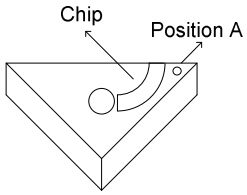

Fig. 4 Tool temperature measurement position (A) by infrared pyrometer

C. Experimental set-up

The standalone temperature measurement work-station consisted of an infrared pyrometer, mounted on the cross slide of the lathe and placed directly over the tool rack face during the cutting tests, and the analysis software mounted on a personal computer. Cutting force, feed force and tool temperature were measured by dynamometer simultaneously. To record the data from dynamometer, a Yokogawa DL-4200 model oscilloscope and written software were used. The total time of sampling is 60000 ms and the total samples are 60 in quantity. The schematic description and photo of experimental set-up are shown in Fig. 5.

Fig. 5 Schematic experimental Set-up

The cutting parameters used in the following experiments are shown in Table I.

TABLE I
CUTTING PARAMETERS FOR DIFFERENT TESTS

Cutting speed (V)	131, 185, 263, 528, 733 (mm/s)
Depth of cut (h)	1.5, 2.1, 2.94, 4.1 (mm)

IV. RESULTS

Temperature field observed on the tool is measured with an infrared camera and compared to simulations for three dimensional tool temperature field which is pertinent to the maximum rake face temperature of the tool from an orthogonal point of view.

A. Temperature in various cutting speeds

In these experiments, the cutting speed (V) is a variable parameter, as indicated in table I, the feed rate and depth of cut are 0.08 mm/rev and 1.5 mm, respectively. The results achieved from infrared pyrometer are illustrated in Fig. 6. It can be seen that in the beginning of the set-up, the temperature is increased with a rather steep slope, and as time progresses the slope of curve decreases and approaches zero.

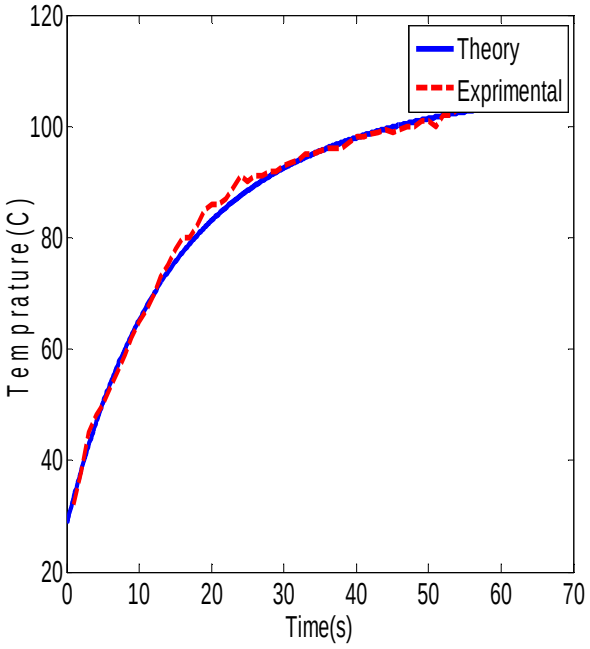

(a)

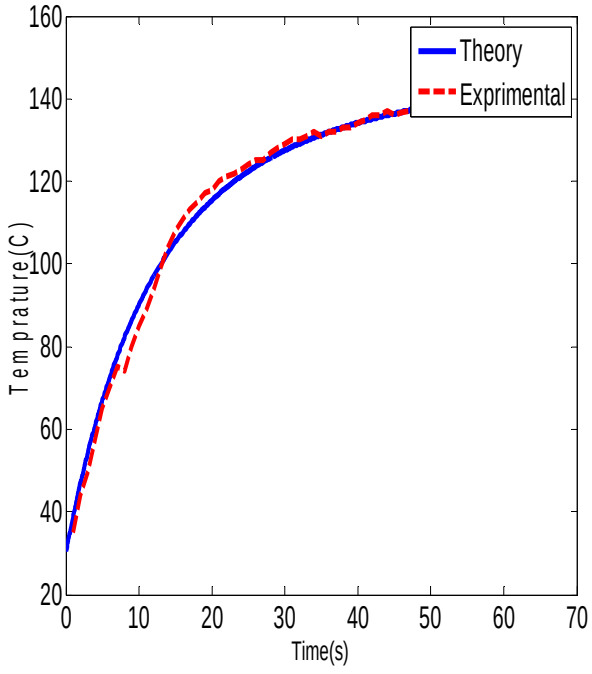

(b)

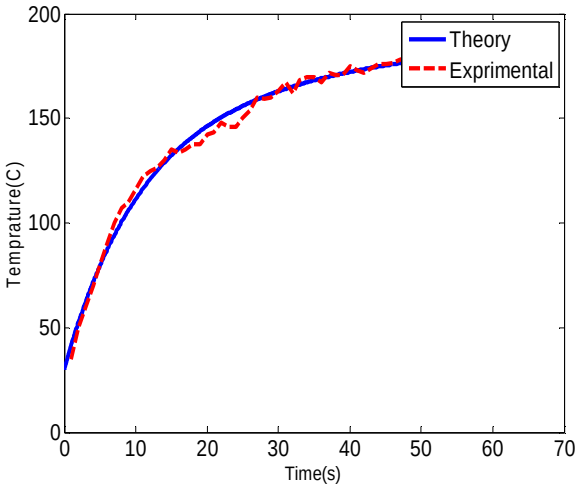

(c)

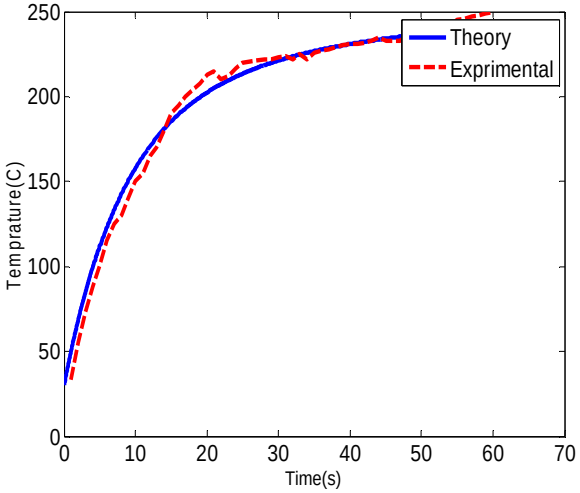

(d)

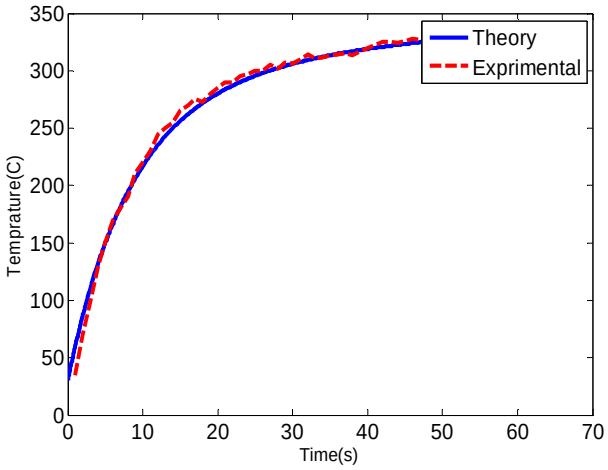

(e)

Fig. 6 F Tool temperature vs. Time in (a) V=131 mm/s, (b) V=185 mm/s, (c) V=263 mm/s (d) V=528 mm/s and (e) V=733 mm/s

B. Tool temperature in various depth of cut

In these tests, the cutting speed and feed rate are 131 mm/s and 0.08 mm/rev, respectively, and the effect of changing depth of cuts on tool temperature is considered according to table 1. The results from the embedded infrared pyrometer are shown in Fig. 1. One of the main points of these experiments demonstrates that the slope of the tool temperature curve decreases intensely, moreover, the effect of depth of cut on tool temperature is less than that of feed rate and cutting speed.

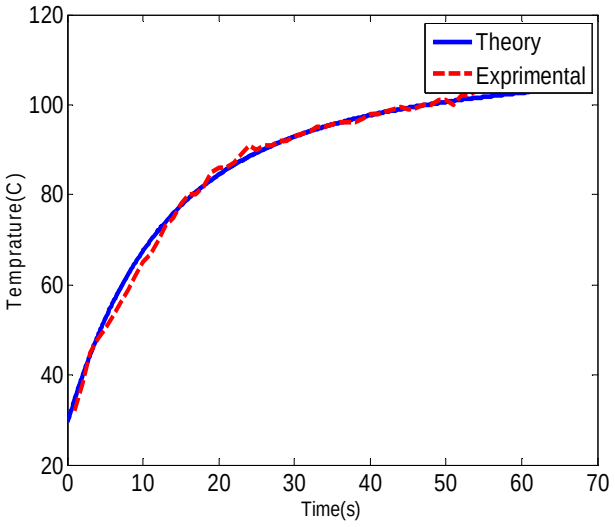

(a)

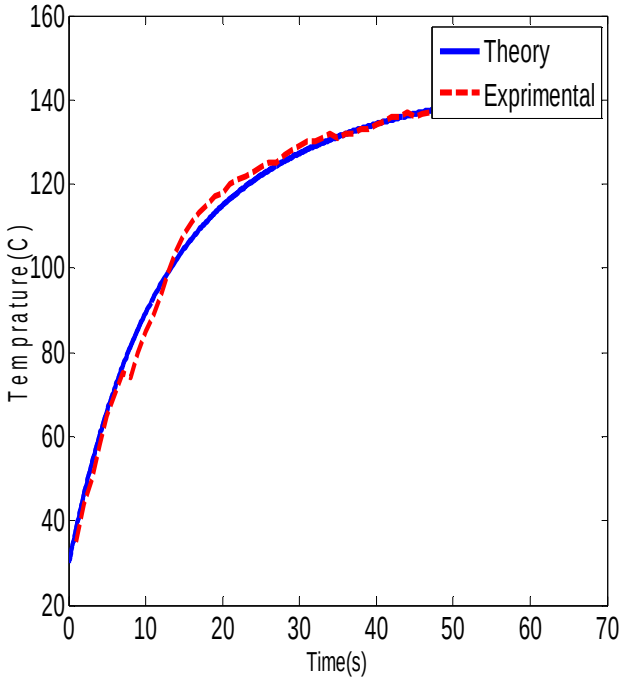

(b)

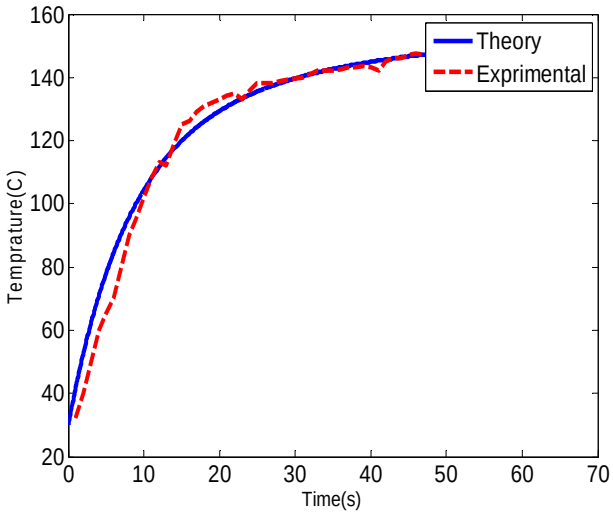

(c)

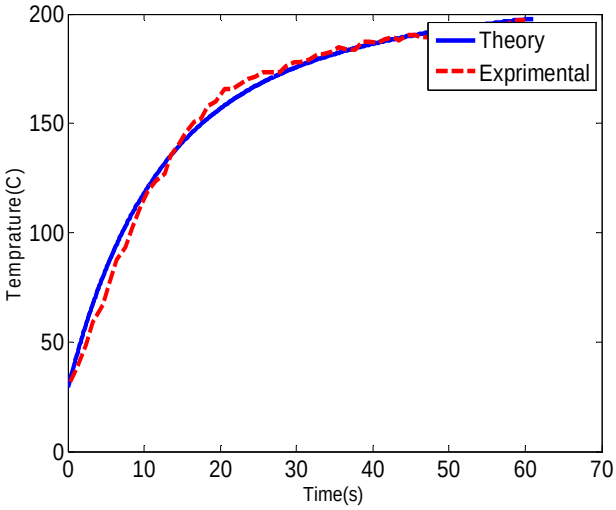

(d)

Fig. 2 Tool temperature vs. Time in (a) h=1.5 mm, (b) h=2.1 mm, (c) h=2.94 mm and (d) h=4.1 mm

V. Conclusion

In this paper, an accurate model of tool is presented and three-dimensional temperature field on tool during machining is computed, and then compared with experimental work on C45 workpiece using carbide cutting tool inserts. The results of experiment can be used as inputs of the residual stress prediction which is one of the other important current topics in the machining research.

Moreover, this work is carried out to obtain the relation between tool temperature and cutting conditions such as cutting speed, feed rate and depth of cut. According to performed experiments, the following results have been obtained:

1) Due to the complexity of machining processes, various measuring techniques should be integrated to obtain temperature.

2) With an increase in the cutting speed, feed rate and depth of cut, the tool temperature is increased and the cutting speed is found to be the most effective parameter in temperature rise, especially in high range of cutting conditions.

3) When the cutting speed, feed rate, and depth of cut are considered, the cutting speed and feed rate were found to be more effective than the depth of cut on tool temperature. By increasing the feed rate and depth of cut more from a specific range, the amount tool temperature approaches to an almost straight line with low slope and the feed rate was found to be more effective than the depth of cut in tool temperature. Therefore, in order to increase the chip removal efficiency, it is better to increase the depth of cut and then increase the feed rate and cutting speed, respectively.

REFERENCES

[1] D. Ulutan, I. Lazoglu, C. Dinc, 2008, "Three-dimensional temperature predictions in machining process using finite difference method," journal of materials processing technology - 2009.

[2] N. Fang, C. Fang, 2007, "Theoretical and experimental investigations of finish machining with a rounded edge tool," J. Mater. Process. Technol. 191, 331–334.

[3] L. Filice, F. Micari, S. Rizzuti, D. Umbrello, 2007a. A critical analysis on the friction modeling in orthogonal machining Int. J. Mach. Tools Manuf. 47, 709–714.

[4] X.J. Ren, Q.X. Yang, R.D. James, L. Wang, 2007. Cutting temperatures in hard turning chromium hard facings with PCBN tooling. J. Mater. Process. Technol. 147, 38–44.

[5] W. Grzesik, M. Bartoszuk, P. Nieslony, 2005, "Finite element modeling of temperature distribution in the cutting zone in turning processes with differently coated tools," Journal of Materials Processing Technology, Vol. 164- 165, pp 1204-1211.

[6] P.C. Wanigaratne, A.D. Kardekar, O.W. Dillon, G. poulachon, I.S. jawahir, 2005, "progressive tool-wear in machining with coated grooved tools and its correlation with cutting temperature," Wear, vol. 259, 1215-122d.

[7] I. Lazoglu, K. Buyukhatipoglu, H. kratz, F. klocke, 2006, "Forces and temperature in hard turning," Mach. Sci. Technol. Vol. 10, pp. 157-179.

[8] N.A. Abukhshim, P.T. Mativenga, M.A. Sheikh, 2006, "Heat generation a temperature prediction in metal cutting: a review and implications for high speed machining," Int. Journal of Machine Tools and Manufacture, Vol. 46 (7-8), pp. 782-800.

[9] G. List, G. Sutter, A. Bouthiche, 2012, "Cutting temperature prediction in high speed machining by numerical modeling of chip formation and its dependence with crater wear," Int. Journal of Mach. Tools and Manufacture, Vol. 54–55, pp. 1-9.

[10] I. Lazoglu, Y. Altintas, 2002. "Prediction of tool and chip temperature in continuous and interrupted machining," International Journal of Machine Tools and Manufacture, Vol.42, 1011-1022.